

## Nonlinear Finite Element Analysis of High Strength Lightweight Concrete Beams

Farked Kais Ibrahim\*

Received on 16/12/2009

Accepted on: 11/3/2010

### Abstract

This research work presents a nonlinear finite element investigation on the behavior of lightweight reinforced concrete beams. This investigation is carried out in order to get a better understanding of their behavior throughout the entire loading history.

The three-dimensional 20-node brick elements are used to model the concrete, while the reinforcing bars are modeled as axial members embedded within the concrete brick elements. The compressive behavior of concrete is simulated by an elastic-plastic work-hardening model followed by a perfectly plastic response, which terminated at the onset of crushing. In tension, a fixed smeared crack model has been used. The effect of some important parameters ( $f'_c$ ,  $r_w$ ,  $a/d$ ) have been investigated to study their influence on the predicted load-deflection curves.

**Keywords:** Nonlinear, Finite Element, Lightweight, Beams.

### التحليل اللاخطي للعتبات الخرسانية الخفيفة الوزن ذات المقاومة العالية باستخدام طريقة العناصر المحددة

#### الخلاصة

تم في هذا البحث اختبار سلوك العتبات الخرسانية الخفيفة الوزن المسلحة ذات المقاومة العالية والمعرضة لاحمال القص باستخدام نموذج التحليل غير الخطي بطريقة العناصر المحددة. هذا النموذج استخدم للحصول على تفهم افضل لتصرف هذه الاعضاء من خلال تاريخ التحميل الكامل. تم استخدام العنصر الطابوقي ذو العشرين عقدة لتمثيل الخرسانة ، اما قضبان التسليح فقد مثلت كعناصر احادية البعد مطمورة في العنصر الخرساني ثلاثي الابعاد ، تم تمثيل تصرف الخرسانة تحت تاثير اجهادات الضغط بالانموذج المرن-اللدن ذو التقوية الانفعالية حيث يتضمن هذا الانموذج افتراض سلوكاً مرناً للخرسانة في مستهل التحميل يعقبه سلوك مرن - لدن عند حدوث التشقق في الخرسانة ، ويستمر تحمل الاجهادات بمعدل انفعال متزايد لحين وصول مرحلة اللدونة التامة، وتنتهي هذه المرحلة بحدوث تهشم في الخرسانة . اما سلوك الخرسانة تحت تاثير اجهادات الشد فقد تم تبني انموذج التشقق المنتشر لتمثيله. تم دراسة تاثير المعاملات المهمة ( $f'_c$ ,  $r_w$ ,  $a/d$ ) على منحنيات الحمل-هطول المتوقع.

### Introduction

Structural lightweight-aggregate concrete made with structural lightweight aggregate as defined in ASTM C 330. The concrete has a minimum 28 day compressive strength of (17 MPa), an

equilibrium density between (1120 and 1920 kg/m<sup>3</sup>), and consists entirely of lightweight aggregate or a combination of lightweight and normal-density aggregate[1]. In the last few years there was an increasing interest in concrete for

heat isolating elements in housing, for bridge structures or other structural elements. In the field of civil engineering, lightweight concrete is used in plates or in slender elements e.g. beams. To construct such structural elements without or with a minimum of shear reinforcement is of major interest.

Due to the application of lightweight aggregate concrete (LWAC), it is possible to save weight transferred to the substructures and foundations of a bridge or a building or a energy-related floating structures and so the construction cost and time could be reduced. These structural applications stimulated more-concentrated research into the properties of lightweight concrete to be used for new and novel applications where high strength and high durability are desirable. Structural high-strength lightweight-aggregate concrete is usually defined as a concrete with a 28-day compressive strength of (40 MPa) or greater [1]. All structural concrete elements such as beams, columns, walls and slabs depend on concrete to resist part of the applied shear force. Since a shear failure is rather sudden and non-ductile, it is imperative that the designer be able to accurately predict the concrete contribution to the shear strength. It is essential to study the shear strength of LWAC structural members to provide engineers with a safe, proven design method [2].

#### **Finite Element Model**

In the present research work, a full three - dimensional finite element idealization has been used. This

idealization gives accurate simulation for geometry, type of failure and location of reinforcing bars. The 20-node quadratic brick element shown in Fig. (1) is adopted to represent concrete.

The reinforcement representation that is used in this study is the embedded representation, Fig. (1). The reinforcing bar is considered to be an axial member built into the concrete element. The reinforcing bars were assumed to be capable of transmitting axial force only.

The numerical integration is generally carried out using the 27(3x3x3) point Gaussian type integration rule.

The nonlinear equations of equilibrium have been solved using an incremental-iterative technique operating under load control. The nonlinear solution algorithm that is used in this research work is the modified Newton-Raphson method in which the stiffness matrix is updated at the 2<sup>nd</sup>, 12<sup>th</sup>, 22<sup>nd</sup>, ...etc. iterations of each increment of loading.

#### **Concrete Model Adopted in the Analysis**

##### **Behavior in Compression**

In compression, the behavior of concrete is simulated by an elastic-plastic work hardening model followed by a perfectly plastic response, which is terminated at the onset of crushing. The growth of subsequent loading surfaces is described by an isotropic hardening rule. A parabolic equivalent uniaxial stress-strain curve has been used to represent the work hardening stage of

behavior and the plastic straining is controlled by an associated flow rule.

The concrete strength under multidimensional state of stress is a function of the state of stress and cannot be predicted by simple tensile, compressive and shearing stress independent of each other. So the the state of stress must be scaled by an appropriate yield criterion to convert it to equivalent stress that could be obtained from simple experimental test. The yield criterion that has been used successfully by many investigators [3,4] can be expressed as

$$f(\{\sigma\})=(\alpha I_1+3\beta J_2)^{0.5}=\sigma_0 \quad \dots(1)$$

where  $\alpha$  and  $\beta$  are material parameters which are dependent on the type of concrete.[5,6].  $I_1$  is the first stress invariant and  $J_2$  is the second deviatoric stress invariant.  $\sigma_0$  is an equivalent effective stress at the onset of plastic deformation which can be determined from a uniaxial compression test.

In a reinforced concrete member, a significant degradation in compressive strength can result due to the presence of transverse tensile straining after cracking. In the present study, Vecchio et, al. models are used for HSC [7] members, which illustrates the use of the reduction factor,  $\lambda$ . The compressive reduction factor,  $\lambda$ , for HSC is given as:

$$\lambda = \frac{1}{1+K_c \cdot K_f} \quad \dots(2)$$

where  $K_c$  is a factor representing the effect of the transverse cracking and straining and  $K_f$  is a factor representing the effect of concrete compressive strength  $f'_c$ .

$$K_c=0.35 (\varepsilon_1/\varepsilon_3-0.28)^{0.8} \quad \dots(3)$$

and

$$K_f = 0.1825 (f'_c)^{0.5} \geq 1.0 \quad \dots(4)$$

where  $\varepsilon_1$  is the tensile strain in the direction normal to the crack and  $\varepsilon_3$  is the compressive strain in the direction parallel to the crack.

According to test results reported in reference [8], Al-Musawi proposed the modulus of elasticity ( $E_c$ ) in terms of compressive strength ( $f'_c$ ) as follows:

$$E_c = 2900 (f'_c)^{0.5} \quad \dots(5)$$

### Behavior in Tension:

In tension, linear elastic behavior prior to cracking is assumed. Cracking is governed by the attainment of a maximum principal stress criterion. A smeared crack model with fixed orthogonal cracks is assumed to represent the cracked sampling point. The post-cracking tensile stress-strain relation, Fig. (2), [9,10] and the reduction in shear modulus with increasing tensile strain Fig. (3),[11] have been adopted in the present work.

According to test results reported in reference [12] the concrete peak value of the tensile stress of high strength reinforced concrete ( $f_t$ ) is proposed in terms of compressive strength ( $f'_c$ ) as follows:

$$f_t = 0.57 (f'_c)^{0.5} \quad \dots(6)$$

### Numerical Examples

#### Description of Test Specimens:

A total of 17 reinforced lightweight concrete beams were tested by Al-Dhalimi [2] under monotonic loading up to failure. In order to check the validity of the present material model, six of these

beams were chosen for this research work to carry out the finite element analysis. These beams were designated WS120, WS220, WS140, WS240, WS340 and WS230. All tested beams had a rectangular section 102\*203mm with different length as shown in Table (1). Fig.(4) shows loading arrangement and reinforcement details.

#### **Finite Element Idealization and Material Properties:**

By making use of symmetry of loading, geometry and reinforcement distribution of the tested beams, only one quarter of each beam will be considered in the numerical analyses. In the present study, the chosen segments were modeled using 4 brick elements. The finite element mesh, boundary conditions, and loading arrangement are shown in Fig.(5). Dimensions, material properties and the additional material and numerical parameters are listed in Table (1). The longitudinal bars were simulated as embedded elements into the brick elements.

The numerical analysis have been generally carried out using the 27-point integration rule and a convergence tolerance of 2 %. All the analysis have been conducted out using 3DNFEA(Three-Dimensional Non-Linear Finite Element Analysis) computer program and the program was coded in FORTRAN-77 language.

#### **Results of Analysis:**

The experimental and numerical load –deflection curves for beams WS120, WS220, WS140, WS240, WS340 and WS230 are shown in Fig.(6). These figures show good agreement for the finite element solution compared with the

experimental results throughout the entire range of behavior. They reveal that both the initial and post-cracking stiffnesses are reasonably predicted. The computed failure loads for all beams are close to the corresponding experimental collapse load as listed in Table (2).

#### **Parametric Studies**

To investigate the effects of some of the material and solution parameters on the nonlinear finite element analysis of lightweight concrete beams, beam WS140 has been chosen to carry out a parametric study. This study helps to clarify the effect of various parameters that have been considered on the behavior and ultimate load capacity of the analyzed beams.

#### **Effect of Grade of Concrete ( $f'_c$ )**

In the present research work, a study was made to investigate the use of lightweight concrete of higher compressive strength. This was achieved by numerically testing an assumed beam with a wide range of concrete compressive strength. This beam is similar in dimensions, arrangement of reinforcement and other details to WS140. The tension stiffening parameters  $\alpha_1$  and  $\alpha_2$  were set equal to 5 and 0.5 respectively. While the shear retention parameters  $\gamma_1$ ,  $\gamma_2$  and  $\gamma_3$  were set equal to 5, 0.99 and 0.15 respectively.

The results of this investigation are shown in Fig. (7). Four grades of concrete were considered in this study. These were (32.6, 45, 65 and 85 MPa). The analysis revealed that the failure was due to concrete crushing for all grades of concrete. Therefore the cracking load and post-cracking stiffness are increased

by increasing concrete compressive strength. The finite element results revealed that an increase up to 100% in ultimate load capacity can be achieved by using compressive strength equal to 85 MPa, compared to a compressive strength of 32.6 MPa.

#### **Influence of Longitudinal Reinforcement ( $\rho_w$ )**

The influence of using different longitudinal reinforcement ratios ( $\rho_w$ ) on the load-deflection curve is investigated. An assumed beam reinforced with various longitudinal reinforcement ratios was numerically tested. The results are shown in Fig. (8). The longitudinal reinforcement ratio varied from 0.900% to 2.305%. The concrete compressive strength and reinforcement yield stress were 32.6 and 738.4 MPa respectively. By studying the predicted response of the beam, it can be seen that the increase in the longitudinal reinforcement ratio leads to a stiffer post-cracking response and significant increase in the ultimate load capacity of the beam. The finite element results revealed that an increase up to 41.86% in ultimate load capacity can be achieved by using longitudinal reinforcement ratio equal to 2.305%, compared to a ratio of 0.9%. Table (3) shows the comparison between cracking and ultimate loads for different amount of  $\rho_w$ .

#### **Influence of Shear Span-Depth Ratio (a/d)**

In order to investigate the influence of using different shear span-depth (a/d) ratio on the behavior of load-deflection curve of the high strength lightweight concrete beam, an assumed beam reinforced with  $\rho_w=2.305\%$ ,  $f_c=65\text{MPa}$  and various shear span-

depth (a/d) ratios were numerically tested. The results are shown in Fig.(9). The shear span-depth (a/d) ratio varied from 1.0 to 4.0.

By studying the predicted response of the beam, it can be seen that the increase in the shear span-depth (a/d) ratio leads to a decrease in the post-cracking stiffness response and a significant decrease in the cracking load and ultimate load capacity of the beam is noticed. The finite element results revealed that an increase up to 312.86% in ultimate load capacity can be achieved by using shear span-depth (a/d) ratio equals to 4.0 compared with using (a/d) ratio equals to 1.0. Table (4) shows the comparison between cracking and ultimate loads for different shear span-depth (a/d) ratios.

#### **Conclusions**

1. The three dimensional nonlinear finite element model used in the present work is capable of simulating the behavior of high strength lightweight concrete beams subjected to monotonic loading. The finite element analysis carried out showed good agreement with the experimental results throughout the entire range of behavior.
2. The increase in concrete compressive strength results in a significant increase in the ultimate load capacity of the beams when the failure is due to concrete crushing.
3. The increase in longitudinal reinforcement ratio was found to increase ultimate load capacity and post-cracking stiffness. An increase up to 41.86% in ultimate load capacity can be achieved by using longitudinal reinforcement ratio of 2.305%.

4. The decrease in shear span – depth (a/d) ratio was found to increase ultimate load capacity and post-cracking stiffness. An increase up to 312.86% in ultimate load capacity for (a/d=1.0) over ultimate load capacity is obtained for (a/d=4.0).

#### References

- [1].ACI Committee 213, "Guide for Structural Lightweight Aggregate Concrete (ACI 213R-03)," American Concrete Institute, Farmington Hills, MI,2003,38 pp.
- [2].Al-Dhalimi, M. K., "Shear Behavior of Porcelinite Aggregate R.C. Beams", PhD Thesis, University of Technology, 2005,146pp.
- [3].Thannon, A. Y., "Ultimate Load Analysis of Reinforced Concrete Stiffened Shells and Folded Slabs Used in Architectural Structures", Ph.D. Thesis, University of Wales, Swansea, 1988.
- [4].Hinton, E. and Owen, D.R.J., "Finite Element Software for Plates and Shells" Pineridge Press, Swansea, 1984.
- [5].Allose, L. E., "Three Dimensional Nonlinear Finite Element Analysis of Steel Fiber Reinforced Concrete Beams in Torsion", M.Sc. Thesis, University of Technology, 1996.
- [6].Clarke, J.L., " Shear strength of lightweight aggregate concrete beams ", Magazine of Concrete Research , Vol.39, No. 141, 1987, PP 205- 213.
- [7].T.Vecchio, F. J., Collins, M. P., and Aspioties, "High Strength Concrete Elements Subjected to Shear", ACI Structural Journal, July-Aug. 1994, pp. 423-433.
- [8].AL-Musawi, J.M., (2004) , " Flexural behavior of porcelinite reinforced concrete beams ", PhD , Thesis, University of Technology, Iraq .
- [9].Al-Shaarbaf, I. A.S., "Three Dimensional Nonlinear Finite Element Analysis of Reinforced Concrete Beams in Torsion", Ph.D. Thesis, University of Bradford, 1990.
- [10].Al-Moussely, B. S., "Three Dimensional Nonlinear Finite Element Analysis for Reinforced Concrete Beams Subjected to Combined Bending and Torsion", M.Sc. Thesis, University of Technology, 1998.
- [11].Naji, J. H., and I.May, "The Effect of Some Numerical and Material Parameters on the Nonlinear Finite Element Analysis of Reinforced Concrete Beams", Proceedings of the Third Arab Engineering Conference, Vol. 1, March 1998, No. 5 , pp. 10-17.
- [12].Bunni , Z. J. , " Shear Strength in High-Strength Reinforced Concrete Beams " , M. Sc. Thesis , University of Technology, Baghdad , 1998 , 105 PP.

**Nomenclature**

$f'_c$	uniaxial compressive strength of concrete.
$f_y$	yield strength of reinforcement
$f_t$	uniaxial tensile strength of concrete
$\alpha_1, \alpha_2$	tension-stiffening parameters
$b$	material constant
$\beta_1$	shear retention factor
$g_1, g_2, g_3$	shear retention parameters
$\lambda$	compressive strength reduction factor of concrete
$\sigma_n$	stress normal to cracked plane.
$\epsilon_n$	strain normal to cracked plane
$\epsilon_{cr}$	cracking strain
$\sigma_{cr}$	cracking stress.

**Table (1) Dimensions, material properties and the additional material and numerical parameters used for Al-Dhalimi beams [2]**

	WS120	WS220	WS230	WS140	WS240	WS340
<b>Concrete</b>						
Shear Span a (mm)	430	430	513	684	684	684
a/d	2.5	2.5	3.0	4.0	4.0	4.0
Effective Depth d	171	171	171	171	171	171
Effective Span Ln	1130	1130	1296	1638	1638	1638
Young's modulus,	14207	14281	15208	16558	15563	16405
Compressive	24	24.25	27.5	32.6	28.8	32
Tensile strength, $f_t$	3.31	2.864	3.08	3.03	3.183	3.087
Poisson's ratio, $\nu$	0.2	0.2	0.2	0.2	0.2	0.2
<b>Main Reinforcement</b>						
Bar Diameter (mm)	2 $\phi$ 12	3 $\phi$ 12	3 $\phi$ 12	2 $\phi$ 12	3 $\phi$ 12	4 $\phi$ 12
Young's modulus,	200000	200000	200000	200000	2000000	200000
Steel ratio $r_w$ (%)	1.297	1.945	1.945	1.297	1.945	2.593
Yield stress $f_y$	738.4	738.4	738.4	738.4	738.4	738.4
<b>Tension-stiffening parameter</b>						
$\alpha_1$	5	5	5	5	5	5
$\alpha_2$	0.4	0.45	0.45	0.5	0.55	0.55
<b>Shear retention parameters</b>						
$\gamma_1$	5	5	5	5	5	5
$\gamma_2$	0.85	0.85	0.9	0.99	0.99	0.99
$\gamma_3$	0.1	0.1	0.1	0.15	0.15	0.15



**Table (2) Comparison between experimental and predicted ultimate loads.**

Beams	Experimental ultimate Load $P_u$ ( kN )	Numerical ultimate Load ( kN )	
		$P_{u,num}$	$P_{u,num.}$ <hr/> $P_{u,exp.}$
WS120	73	73	1.000
WS220	73	80	1.096
WS230	65	64	0.985
WS140	56	53	0.946
WS240	58	59	1.017
WS340	55	53	0.964

**Table (3) Comparison between cracking and ultimate loads for different amount of longitudinal reinforcement ratio.**

$\rho_w$ %	Numerical Cracking Load ( kN )	Numerical Ultimate Load ( kN )
<b>0.9</b>	8	43
<b>1.458</b>	12	53
<b>2.305</b>	18	61



**Table (4) Comparison between cracking and ultimate loads for different shear span-depth (a/d) ratio.**

a/d	Numerical Cracking Load ( kN )	Numerical Ultimate Load ( kN )
1	51	289
1.5	41	260
2.0	20	245
2.5	10	171
3.0	10	140
3.5	8	101
4.0	8	70

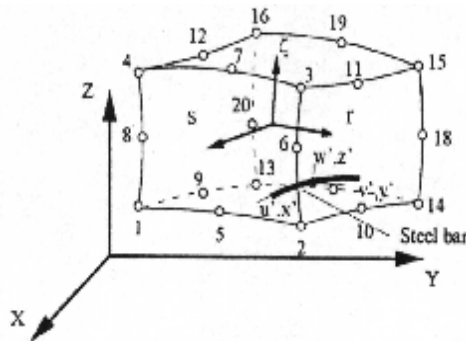


**Figure (1) The twenty-node brick element.**

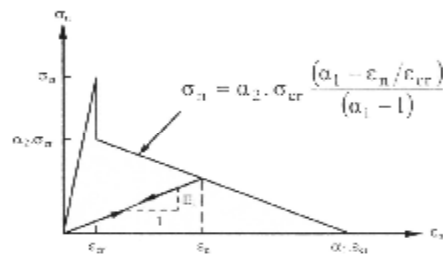


**Figure (2) Post-cracking models for cracked concrete.**

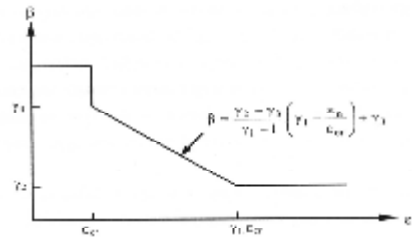


Figure (3) Shear retention model for cracked concrete.

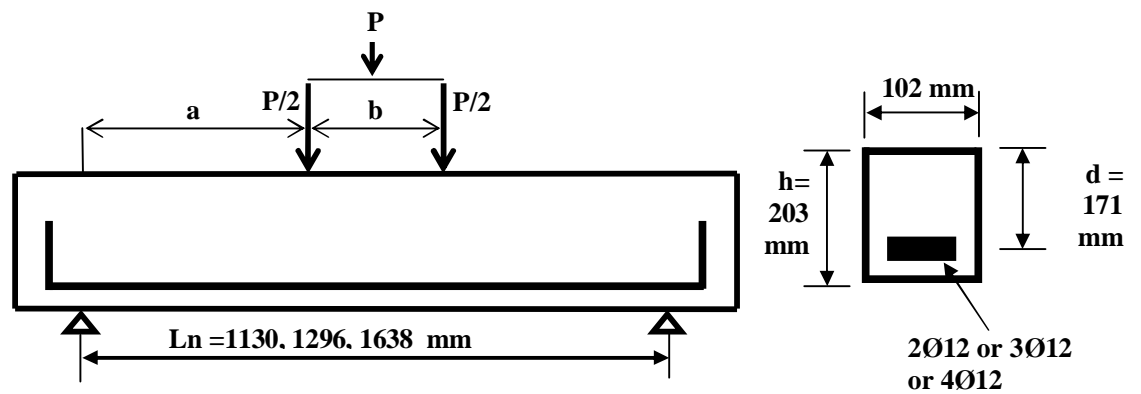


Figure (4) Dimensions and reinforcement details of Al-Dhalimi beams[2].

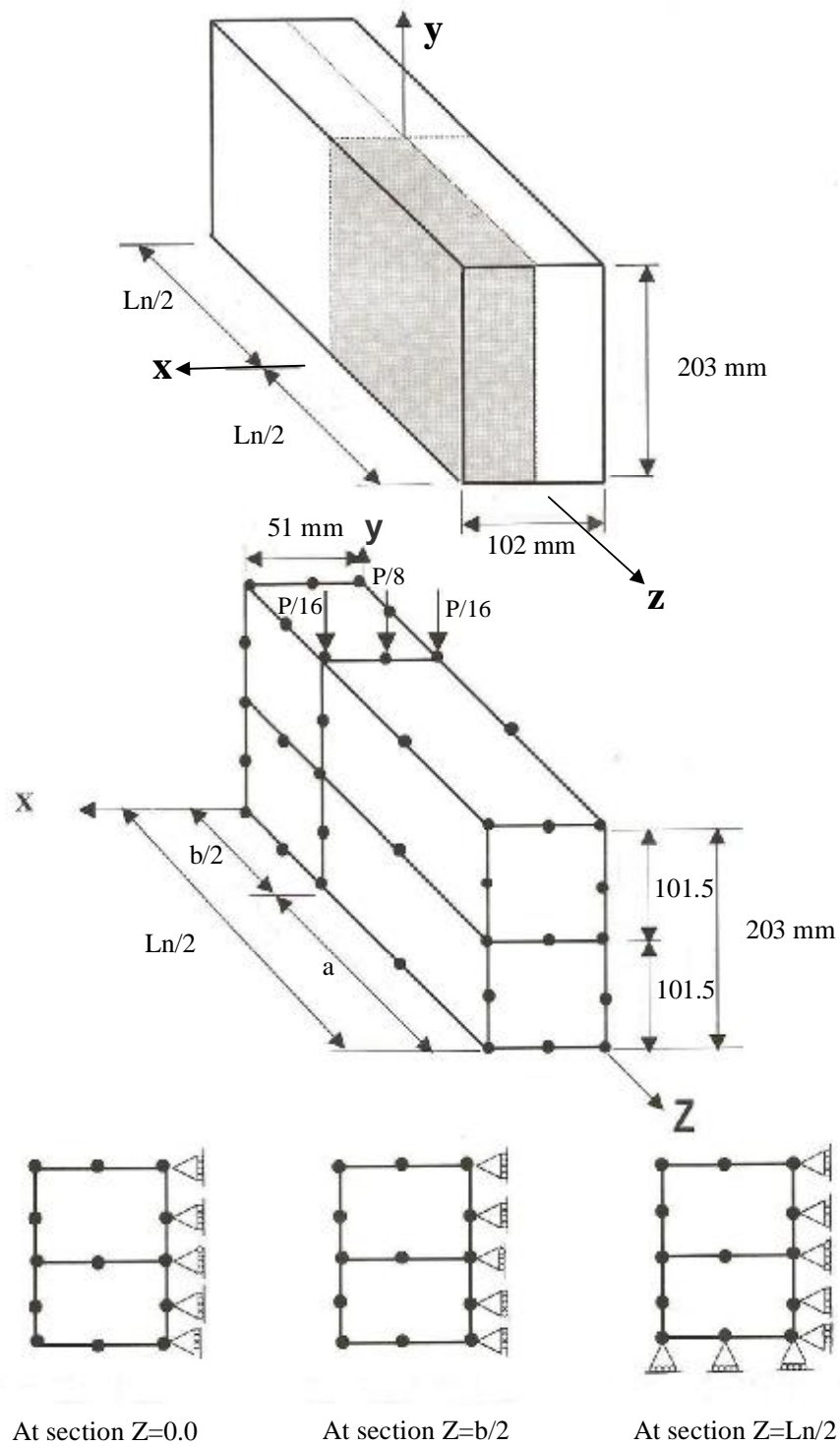


Figure (5) Finite element mesh, boundary and symmetry conditions used for a typical tested beams

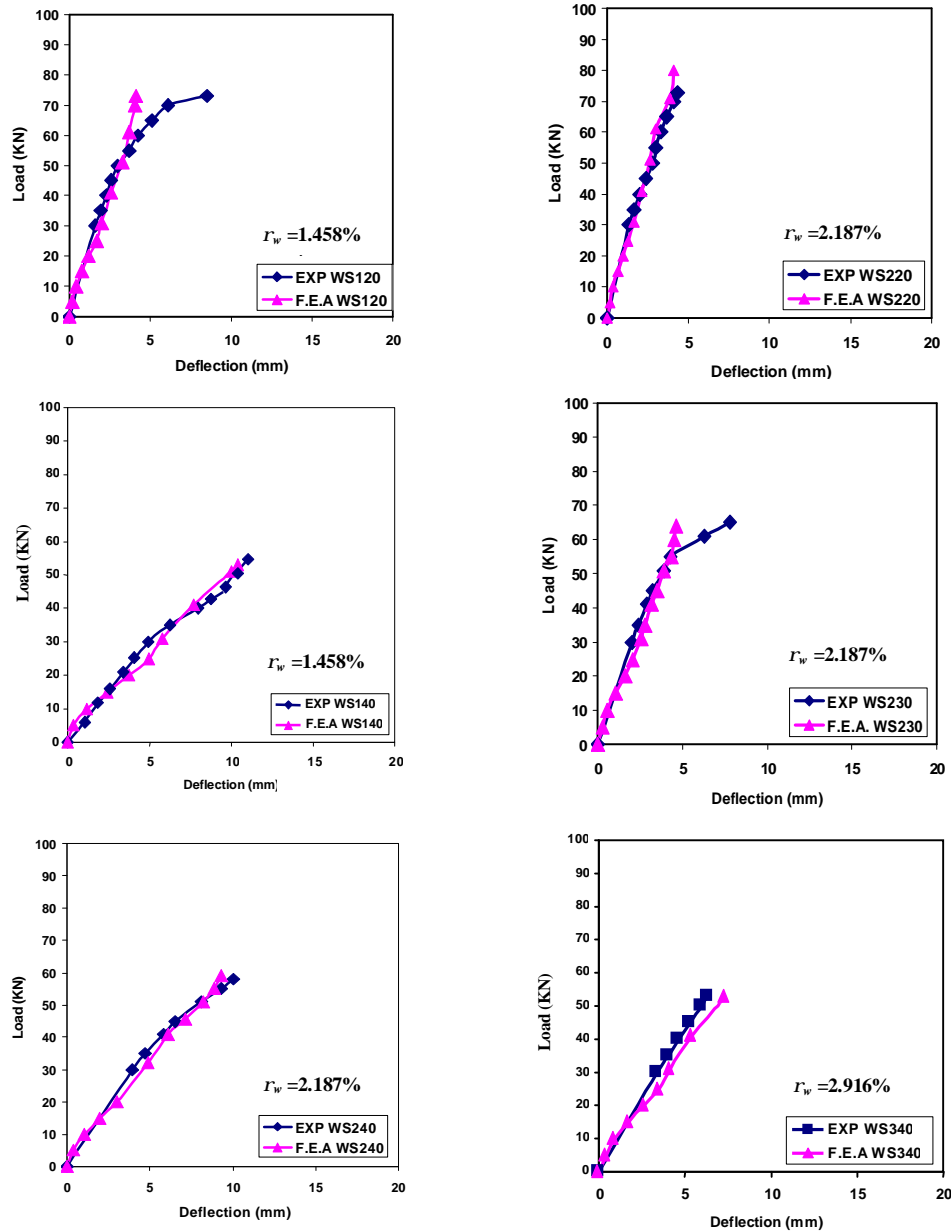


Figure (6) Al-Dhalimi beams, analytical and experimental load-deflection curves

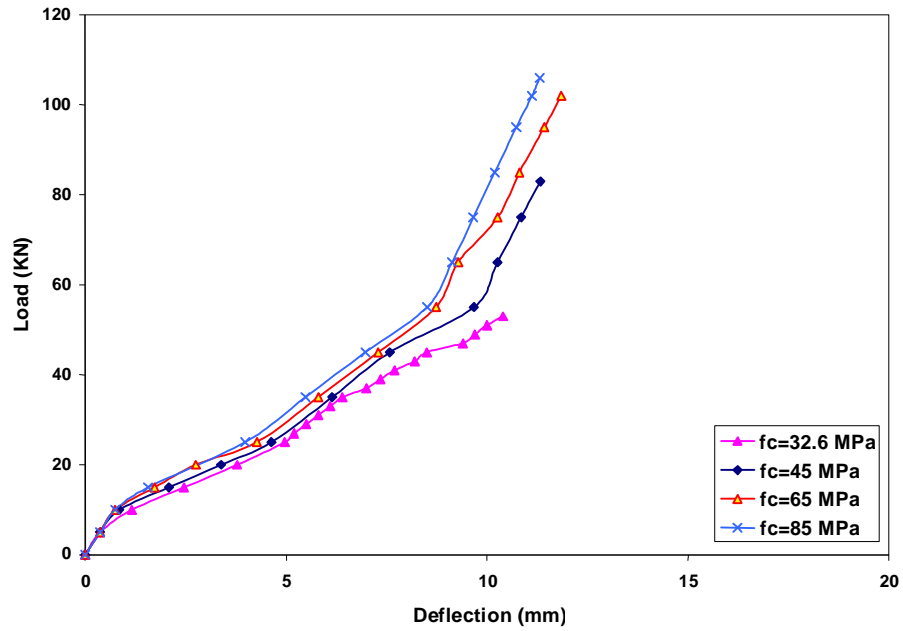


Figure (7) Effect of concrete grade on the load-deflection behavior for beam WS140.

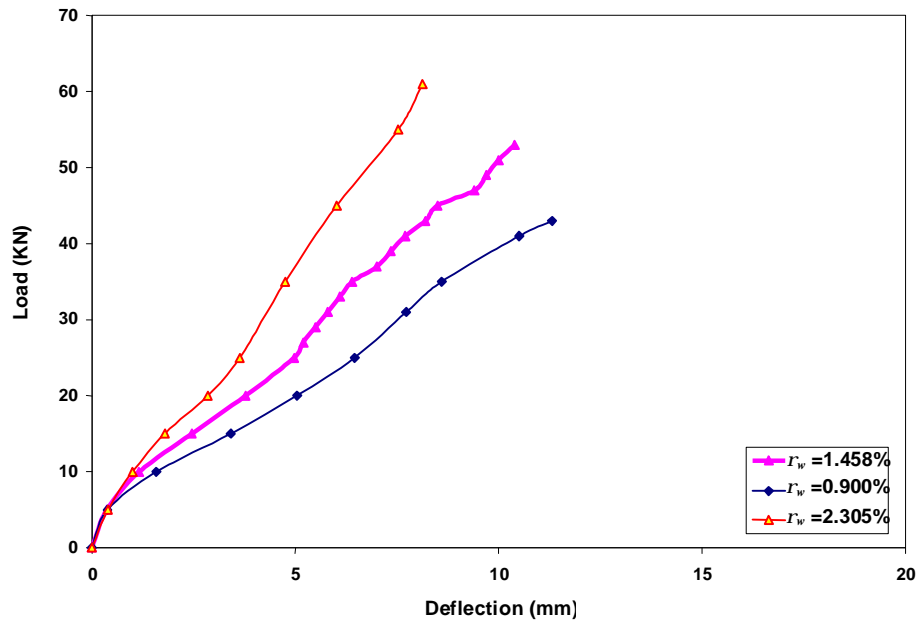


Figure (8) Effect of variation in the longitudinal reinforcement ratio on the load-deflection curve of beam WS140 with a/d=4.

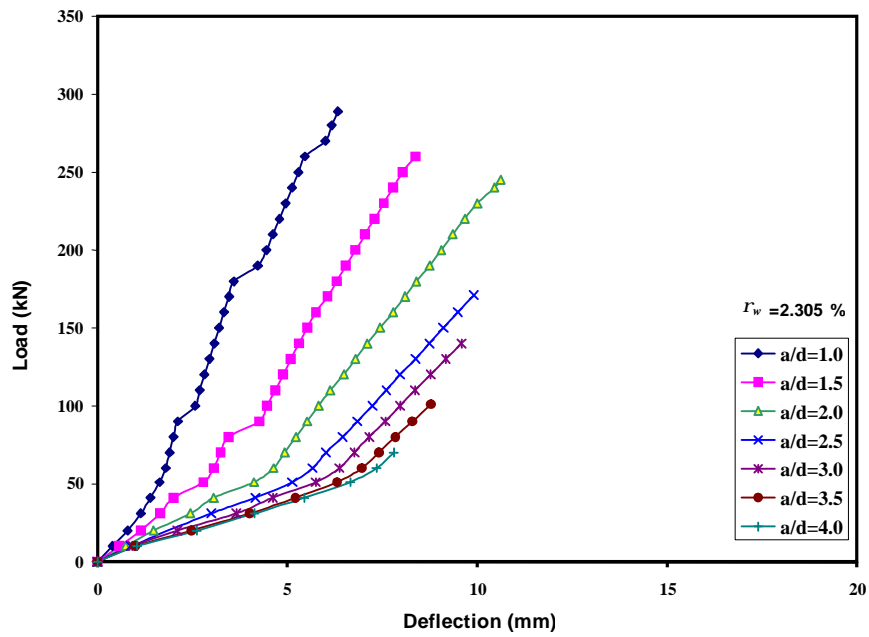


Figure (9) Influence of shear span depth ( $a/d$ ) ratio on load- deflection curve of beam Ws 140 with  $f'c = 65$  MPa